

Influenced of Cu^{2+} Doped on Structural, Morphological and Optical Properties of $\text{Zn-Mg-Fe}_2\text{O}_4$ Ferrite Prepared by Sol-Gel Method

Badawi M. Ali^{1*}, Yousef A. Alsabah^{1,2,3}, Mohamed A. Siddig^{1,4}, Abdelrahman A. Elbadawi^{1,5}, Abdalrawf I. Ahmed¹, Abdulmajid A. Mirghni⁶

¹Department of Physics, Faculty of Science and Technology, Al Neelain University, Khartoum, Sudan

²Research Chair in Laser Diagnosis of Cancers, College of Science, King Saud University, Riyadh, Kingdom of Saudi Arabia

³Department of Physics, Faculty of Education and Applied Science, Hajjah University, Hajjah, Yemen

⁴Department of Physics, Faculty of Science, Albaha University, Albaha, Kingdom of Saudi Arabia

⁵Faculty of Basic Studies, Future University, Khartoum, Sudan

⁶Department of Physics, Faculty of Education, Al Fashir University, Al Fashir, Sudan

Email: *alibadwi07@gmail.com

How to cite this paper: Ali, B.M., Alsabah, Y.A., Siddig, M.A., Elbadawi, A.A., Ahmed, A.I. and Mirghni, A.A. (2020) Influenced of Cu^{2+} Doped on Structural, Morphological and Optical Properties of $\text{Zn-Mg-Fe}_2\text{O}_4$ Ferrite Prepared by Sol-Gel Method. *Advances in Nanoparticles*, 9, 49-58.
<https://doi.org/10.4236/anp.2020.92004>

Received: December 25, 2019

Accepted: March 23, 2020

Published: March 26, 2020

Copyright © 2020 by author(s) and Scientific Research Publishing Inc.

This work is licensed under the Creative Commons Attribution International License (CC BY 4.0).

<http://creativecommons.org/licenses/by/4.0/>



Open Access

Abstract

The $\text{Zn}_{0.5}\text{Cu}_x\text{Mg}_{0.5-x}\text{Fe}_2\text{O}_4$ (where $x = 0.0, 0.1, 0.2, 0.3$ and 0.4) was prepared by sol-gel route and characterized in detail in terms of their structural, morphological, elemental and optical properties as a function of Cu concentration. X-ray diffractometer (XRD) results confirmed the formation of cubic spinel-type structure with average crystallized size in the range of 30.56 to 40.58 nm. Lattice parameter was found to decrease with Cu concentration due to the smaller ionic radius of Cu^{2+} ion. The HR-SEM images show morphology of the samples as prismatic shaped particles in agglomeration. The elemental dispersive X-ray Spectroscopy (EDX) confirmed the elemental composition of the as-prepared spinel ferrite material with respect to the initial concentration of the synthetic composition used for the material. The Fourier transform infrared (FTIR) spectroscopy confirmed the formation of spinel ferrite and showed the characteristics absorption bands around 463, 618, 876, 1116, 1442, 1622 and 2911 cm^{-1} . The energy band gap was calculated for the samples were found to be in the range of 4.87 to 5.30 eV.

Keywords

FTIR, Nano Ferrite, SEM, UV-Vis, XRD, $\text{Zn-Mg-Fe}_2\text{O}_4$ Ferrite

1. Introduction

Ferromagnetism likewise spinel ferrites has general chemical formula MFe_2O_4 (where M is a divalent metal ion of the transition metal elements, such as Mn, Fe, Co, Ni or Cu, Zn, Mg or Cd) [1]. These metals consider as an important and promising material which is widely used for various applications according to their outstanding electronic, optical, magnetic, and catalytic properties [2]. The spinel ferrite has three different types of spinels that are determined by the preference of cation occupancy for A and B-sites, namely normal spinel ferrite, inverse spinel ferrite and intermediate spinel ferrite. Typical examples for these categories are bulk zinc ferrite ($ZnFe_2O_4$) for normal spinel ferrite, copper ferrite ($CuFe_2O_4$) for inverse spinel ferrite and magnesium ferrite ($MgFe_2O_4$) for intermediate spinel ferrite [3] [4] [5]. Ferrites based engineering materials have unique physical and chemical properties. Properties of ferrite are dependent upon several factors, such as composition of preparation, and doping of different cations, sintering temperature, sintered density, a grain size and distribution [6] [7]. Spinel ferrite plays an important role in a variety of technical fields, for example, ferrites have been used in Telecommunication, Digital memories for Computers, Channel filters, satellite communications memory, television industry, audio applications, satellite communications and radar [8] [9]. Doping ferrite as a new substituting method is an important class of materials. Spinel ferrites are examples for doping ferrites [10]. Several synthetic routes were employed for the development of aforementioned mixed ferrite system, namely sol-gel, co-precipitation, hydrothermal and the auto-emulsion methods [11].

The aims of this work are to study the effect of Cu ($x = 0.0, 0.1, 0.2, 0.3,$ and 0.4) doped $ZnMgFe_2O_4$ nanocrystalline. The morphology and optical properties of the samples that prepared using sol-gel method were investigated. Different techniques were used such as X-ray diffractometer (XRD), elemental dispersive X-ray Spectroscopy (EDX), Scanning electron microscope (SEM), Fourier transform infrared (FTIR) spectroscopy, UV-Vis, Spectroscopes.

2. Experimental and Method

Samples $ZnMgFe_2O_4$, $CuFe_2O_4$, $MgFe_2O_4$ and $Zn_{0.5}M_s K_{0.5-x}Fe_2O_4$ where M_s is Cu, $K_{0.5-x}$ is Mg and ($X = 0.0, 0.1, 0.2, 0.3, 0.4$) were prepared by using sol-gel the auto combustion method [12]. High purities of zinc nitrate [$Zn(NO_3)_2 \cdot 6H_2O$ (96%)], Copper nitrate [$Cu(NO_3)_2 \cdot 3H_2O$ (99%)], magnesium nitrate [$Mg(NO_3)_2 \cdot 6H_2O$ (99%)], Ferric nitrate [$Fe(NO_3)_3 \cdot 9H_2O$ (98%)] and Sodium hydroxide (96%) were used as raw materials. The amount of metal nitrates in Cactus oil was Homogenous and separatism of metal ions were achieved by the use of sodium hydroxide. A required amount of sodium hydroxide added into the solution in order to modify pH value to about 7. The solution was constantly stirred for an hour at room temperature using magnetic stirrer. The obtained sol was heated at $80^\circ C$ in a magnetic stirrer to condensate into a gel, and then ignited in a self-propagating combustion manner to form a fluffy loose powder. Finally, the

powders were grained by agate motor and the pellets were finally sintered at 750°C for 4 h in a programmable furnace to remove any organic material present in samples.

Crystal structure of samples were investigated using X-ray diffraction (XRD) techniques—the shimadzu 60,000 X-ray diffract meter—with Cu-K α radiation of a wavelength of $\lambda = 1.5406 \text{ \AA}$ [13]. At room temperature, with nickel filter operating at 40 KV, 40 mA the data collected for the 2θ in 0.02-step size and five-second count in 0.02-step size and five-second count time 20 - 80 range. The MDI jade 0.5 programs used for the XRD data analysis. The crystallite size (D) calculated by Scherer equation [14].

“The SEM images were obtained on a Zeiss Ultra plus 55 field emission scanning electron microscopy (FE-SEM) (Carl Zeiss, Oberkochen, Germany) operated an accelerating voltage of 2.0 KV” investigated the morphology powder and analysis the elements energy dispersive X-ray Spectroscopy (EDX). The transmittance mode investigated for the sample by a (satellite FTIR 5000 of the wavelength rang of 400 to 4000 cm^{-1}) [14] at room temperature. A Fourier transform infrared spectroscopy collected by KBr pellet method, the material mixed with KBr of ratio 1:100 for FTIR measurement between 400 and 2000 cm^{-1} [15] [16].

The UV-Visible absorption was investigated by UV Mini 1240 manufactured by Shimadzu company—Japan. Hydrochloric acid HCL was used as a reference for 100% absorbance [17].

3. Results and Discussion

3.1. Structural Analysis

The results of samples ferrites of $\text{Zn}_{0.5}\text{Cu}_x\text{Mg}_{0.5-x}\text{Fe}_2\text{O}_4$ with ($X = 0.0, 0.1, 0.2, 0.3,$ and 0.4) are illustrated in **Figure 1**. The spectra showed the presence of peaks that correspond to (002), (110), (111), (310), (112), and (002) planes, where highly intense peak at (002) plane confirms cubic spinel structure of as-prepared material [11]. The lattice parameters constants (a) are found to decrease from (8.906 - 8.35) \AA as the value of X increases. The particle size of the nanocrystalline varies from (30.56 - 40.58) nm. It can be noticed that the lattice constant decrease with increasing Cu concentration. This is maybe due to the fact that Cu^{2+} ions (0.73 \AA) is larger than that of the Mg^{2+} ions (0.71 \AA) [7]. Addition of Cu^{2+} at the expense of Mg^{2+} in the ferrite is expected to decrease the lattice constant. The lattice constant (a), crystallite size (D), volume (v), space group, and relative density values of all the compositions are tabulated in **Table 1**.

The particle size of the nanocrystalline varies from (30.56 to 40.58) nm for different compositions. The observed variation in crystallite size of Cu^{2+} substituted Zn Mg ferrite supports the observed lattice constant variation results. From **Table 1**, it can be observe that the density increase with increasing Cu^{2+} content, exhibiting maximum 6.1 g/cm^{-3} for ($X = 0.4$). As magnesium has larger atomic weight than copper, the density of the sample without Cu doping ($X = 0$)

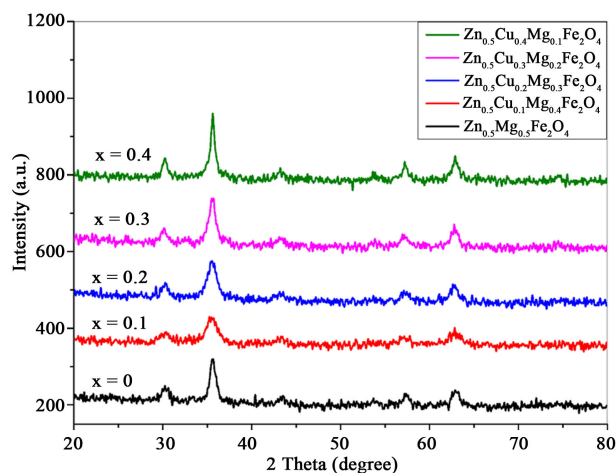


Figure 1. XRD pattern for Cu-doped $Zn_{0.5}Cu_xMg_{0.5-x}Fe_2O_4$ samples.

Table 1. Crystallite size (D), Lattice constant (a), Volume (v) Space group and density of $Zn_{0.5}Cu_xMg_{0.5-x}Fe_2O_4$ Nano-ferrites: where (X = 0.0, 0.1, 0.2, 0.3, 0.4).

Samples	Crystallite Size (nm)	Lattice constant (Å)	Volume (nm ³)	Space group	Density (g/cm ⁻³)
$Zn_{0.5}Mg_{0.5}Fe_2O_4$	30.56	8.906	276.48	Fd-3m (227)	2.550
$Zn_{0.5}Mg_{0.4}Cu_{0.1}Fe_2O_4$	32.66	8.906	276.48	Fd-3m (227)	2.550
$Zn_{0.5}Mg_{0.3}Cu_{0.2}Fe_2O_4$	33.72	8.906	276.48	Fd-3m (227)	2.550
$Zn_{0.5}Mg_{0.2}Cu_{0.3}Fe_2O_4$	37.96	8.405	588.90	Fd-3m (227)	5.62
$Zn_{0.5}Mg_{0.1}Cu_{0.4}Fe_2O_4$	40.58	8.35	582.18	Fd-3m (227)	6.100

is observed to be lower than that of Cu^{2+} doping (X = 0.4) sample. The values of weight and atomic are given in **Table 2** [11]. The increase in density may be due to the ionic of constituent ions.

After analyzing the XRD data, the structural studies showed that all the samples prepared through the sol-gel method are single phase of a face-centered cubic (FCC) spinel and a symmetry structures with space group (SG: Fd-3m).

3.2. Morphological Properties

The morphological characteristics of the gained $Zn_{0.5}Mg_{0.5-x}Cu_xFe_2O_4$ (X = 0.0, 0.1, 0.2, 0.3 and 0.4) nanoparticles are discovered with the high resolution Scanning electron microscopy and are shown in **Figure 2**. HR-SEM images of $Zn_{0.5}Cu_xMg_{0.5-x}Fe_2O_4$ samples **Figures 2(a)-(e)** reveal that all the samples are displayed a close arrangement of homogeneous nanoparticles with prismatic shape. **Figure 2(a)** shows the presence of pure $Zn_{0.5}Mg_{0.5}Fe_2O_4$ nanoparticles, and **Figures 2(b)-(e)** shows the images of Cu-doped Zn Mg ferrite nanoparticles, which are homogeneous and agglomerated with diameter ranging from 1.9 to 2.4 nm. The SEM images of **Figures 2(a)-(e)** of $Zn_{0.5}Cu_xMg_{0.5-x}Fe_2O_4$ reveal that the particle's size and morphology of nanoparticles are an agglomerated due to the presence of magnetic interactions between the particles [18].

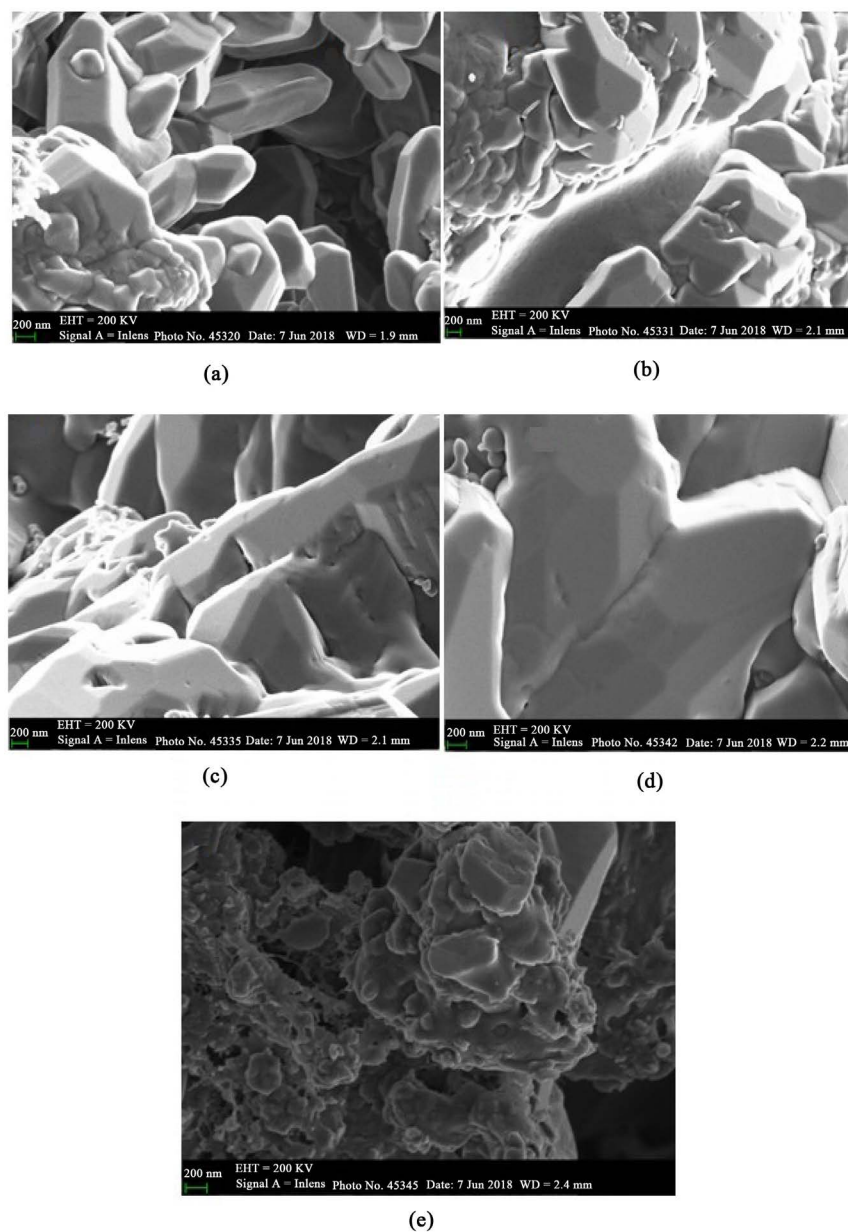


Figure 2. (a)-(e) FE-SEM images of (a) $\text{Zn}_{0.5}\text{Mg}_{0.5}\text{Fe}_2\text{O}_4$; (b) $\text{Zn}_{0.5}\text{Cu}_{0.1}\text{Mg}_{0.4}\text{Fe}_2\text{O}_4$; (c) $\text{Zn}_{0.5}\text{Cu}_{0.2}\text{Mg}_{0.3}\text{Fe}_2\text{O}_4$; (d) $\text{Zn}_{0.5}\text{Cu}_{0.3}\text{Mg}_{0.2}\text{Fe}_2\text{O}_4$; (e) $\text{Zn}_{0.5}\text{Cu}_{0.4}\text{Mg}_{0.1}\text{Fe}_2\text{O}_4$ samples.

Table 2. EDX analysis (weight % and atomic %) of $\text{Zn}_{0.5}\text{Mg}_{0.5-x}\text{Cu}_x\text{Fe}_2\text{O}_4$ ($X = 0.0 - 0.4$).

Composition	X = 0.0		X = 0.1		X = 0.2		X = 0.3		X = 0.4	
	Weight %	Atomic %								
O	71.49	75.01	67.95	67.39	69.51	67.80	69.75	68.81	60.14	57.61
Fe	11.36	3.41	6.23	1.77	5.89	1.65	4.71	1.33	6.00	1.65
Mg	0.16	0.11	0.54	0.35	0.07	0.08	0.12	0.08	0.24	0.15
Cu	-	-	0.22	0.06	0.61	0.15	1.78	0.44	1.62	0.39
Zn	0.25	0.06	0.71	0.17	1.48	0.64	0.18	0.04	0.11	0.03

3.3. EDX Spectroscopy Analysis

The EDX analysis is carried out to obtain an indication of the amount of $Zn_{0.5}Cu_xMg_{0.5-x}Fe_2O_4$ series ($X = 0.0, 0.1, 0.2, 0.3$ and 0.4) are shown in **Figures 3(a)-(e)** and **Table 2**. The EDX spectroscopy is found to support the chemical composition of ferrites formations. The analysis fitting coefficients of iron, copper, Magnesium, Zinc, ferric, and oxygen of the individual nano-ferrite are generated by energy dispersive of SEM. From **Figure 3(a)** shows that the peak of Fe, Zn, Mg and O elements in pure $Zn_{0.5}Mg_{0.5}Fe_2O_4$ and **Figures 3(b)-(e)** shows the peaks of (Zn), (Cu), (Fe), (Mg) and (O) elements for Cu-doped Zn Mg Fe_2O_4 which is in agreement with (XRD) results. The presence of atoms C, Al, Si maybe attributed to carbon-coating for SEM measurement which was applied prior to EDX measurement.

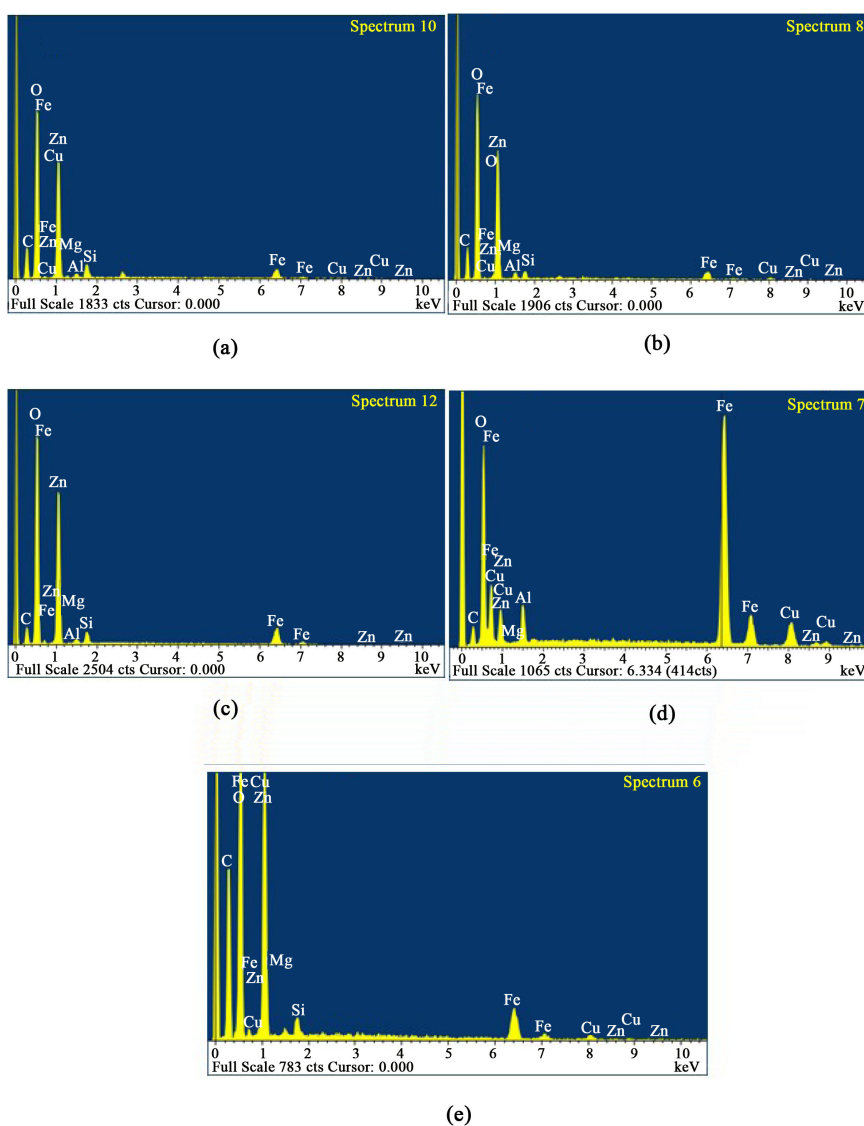


Figure 3. (a)-(e) EDX spectra of (a) $Zn_{0.5}Mg_{0.5}Fe_2O_4$; (b) $Zn_{0.5}Cu_{0.1}Mg_{0.4}Fe_2O_4$; (c) $Zn_{0.5}Cu_{0.2}Mg_{0.3}Fe_2O_4$; (d) $Zn_{0.5}Cu_{0.3}Mg_{0.2}Fe_2O_4$; (e) $Zn_{0.5}Cu_{0.4}Mg_{0.1}Fe_2O_4$ samples.

3.4. Fourier Transform Infrared Spectroscopy

FT-IR spectra of investigating samples of $Zn_{0.5}Cu_xMg_{0.5-x}Fe_2O_4$ ferrites with ($X = 0.0, 0.1, 0.2, 0.3, 0.4$) is shown in **Figure 4** which are observed in the range of $4000 - 400 \text{ cm}^{-1}$. All the samples show that many peaks which are responsible for different functional groups appear in the range $3600 - 1200 \text{ cm}^{-1}$. Small peak at 3426 cm^{-1} indicated the presence O-H group, and C-H bending appears in $850 - 1200 \text{ cm}^{-1}$. Two broad metal–oxygen bands are seen in the IR spectra of all spinel's and ferrites in particular. The highest ν_1 is attributed to the intrinsic stretching vibrations of the metal at the tetrahedral site the lowest ν_2 band corresponds to the octahedral stretching vibrations [19]. The highest ν_1 band is generally observed in the range $650 - 600 \text{ cm}^{-1}$ corresponds of intrinsic stretching vibrations of the metal at the tetrahedral site, whereas the lowers band (ν_2), usually observed in the range $450 - 380 \text{ cm}^{-1}$, is assigned octahedral, metal stretching, the spectra showed prominent bands near 3426 cm^{-1} and 1600 cm^{-1} which were attributed to the stretching modes and H-O-H bending vibrations of the free or absorbed water.

3.5. Uv.vis Result

The optical absorption technique can be utilized for an examination of the optically induced transitions and can supply information about the energy gap in crystalline and Nano-crystalline materials. **Figure 5** show UV-vis absorption spectra for the present study in particular the relation between optical absorption and wavelength of nanoparticle samples at room temperature. The absorption peaks of $Zn_{0.5}Cu_xMg_{0.5-x}Fe_2O_4$ are found to be 255, 243, 234, 249, and 240 nm for ($X = 0.0, 0.1, 0.2, 0.3, \text{ and } 0.4$) respectively. The optical band gap was obtained from the analysis of the spectral dependence of the absorption near the absorption edge $E_g = 1242/\lambda$. Regarding the optical transition arising from photons of energy ($h\nu > E_g$), the present optical data can be determined according to the following relationship of the near optical absorption, That estimated values of the band gap of $Zn_{0.5}Cu_xMg_{0.5-x}Fe_2O_4$ ($X = 0.0, 0.1, 0.2, 0.3, \text{ and } 0.4$)

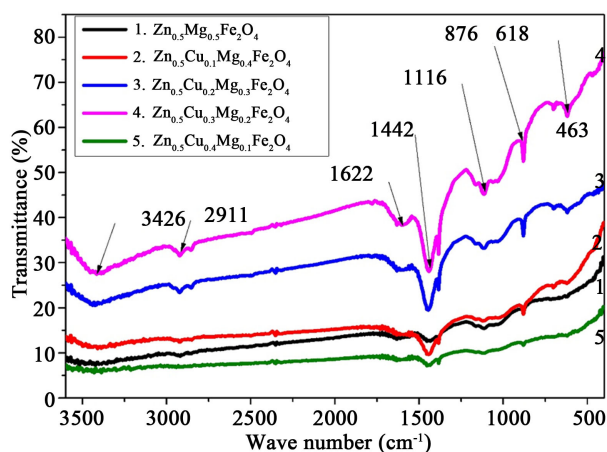


Figure 4. FT-IR for Cu-doped Zn Mg Fe₂O₄.

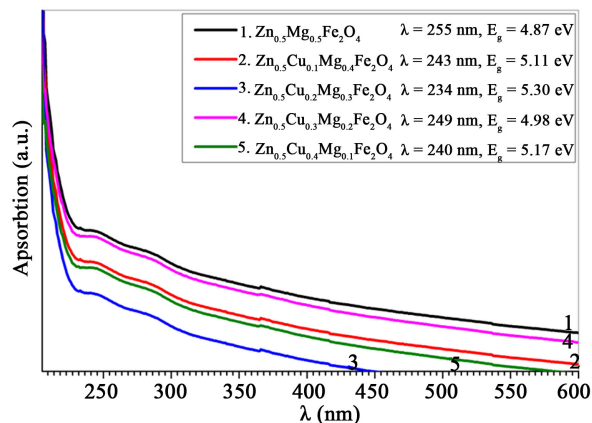


Figure 5. (a) UV-vis Absorbance spectrum of $\text{Zn}_{0.5}\text{Cu}_x\text{Mg}_{0.5-x}\text{Fe}_2\text{O}_4$ samples.

nanoparticles are 4.87, 5.11, 5.30, 4.98 and 5.17 eV in the same order as in **Figure 5** for $X = 0.0$ to $X = 0.4$. The results of the optical energy band gap of sample series indicated that they can be classified as insulator materials [20] [21].

4. Conclusion

$\text{Zn}_{0.5}\text{Cu}_x\text{Mg}_{0.5-x}\text{Fe}_2\text{O}_4$ series were synthesized by sol-gel route and the structural and morphological properties were studied by XRD and SEM. The samples were found to be cubic spinel-type structure with average crystallite size in the range of 30.56 to 40.58 nm. In the same way, the FE-SEM images showed morphology of the samples as prismatic shaped particles in agglomeration. EDX result confirmed the Elemental composition of the as-prepared spinel ferrite to the initial concentration of the synthetic composition used. The FTIR spectroscopy confirmed the formation of spinel ferrite. The energy band gap was calculated for samples were found to be in the insulator range.

Acknowledgements

I would like to thank the department of physics Al-Neelain University, particularly Laboratory of materials for supporting we carry out this paper. Thanks are also extended to the Physics Department, Pretoria University, South Africa for analyzing the Samples through SEM and EDX measurement.

Conflicts of Interest

The authors declare no conflicts of interest regarding the publication of this paper.

References

- [1] Pereira, C., Pereira, A.M., Fernandes, C., Rocha, M., Mendes, R., Fernández-García, M.P. and Freire, C. (2012) Superparamagnetic MFe_2O_4 ($\text{M} = \text{Fe}, \text{Co}, \text{Mn}$) Nanoparticles: Tuning the Particle Size and Magnetic Properties through a Novel One-Step Coprecipitation Route. *Chemistry of Materials*, **24**, 1496-1504. <https://doi.org/10.1021/cm300301c>

- [2] Hassan, A.L. and Maki, S.L. (2017) Structural and Optical Properties of Copper-Doped Cobalt Oxide Thin Films Prepared by Spray Pyrolysis. *International Journal of Engineering Sciences Research Technology*, **6**, 527-535.
- [3] Jamile, M.T., Ahmad, J., Bukhari, S.H., Sultan, T., Akhter, M.Y., Ahmad, H. and Murtaza, G. (2017) Effect on Structural and Optical Properties of Zn-Substituted Cobalt Ferrite CoFe_2O_4 . *Journal of Ovonic Research*, **13**, 45-53.
- [4] Agouriane, E., Rabi, B., Essoumhi, A., Razouk, A., Sahlaoui, M., Costa, B.F.O. and Sajieeddine, M. (2016) Structural and Magnetic Properties of CuFe_2O_4 Ferrite Nanoparticles Synthesized by Co-Precipitation. *Journal of Materials and Environmental Science*, **7**, 4116-4120.
- [5] Deraz, N.M. and Abd-Elkader, O.H. (2015) Structural, Morphological and Magnetic Properties of $\text{Zn}_{0.5}\text{Mg}_{0.5}\text{Fe}_2\text{O}_4$ as Anticorrosion Pigment. *International Journal of Electrochemical Science*, **10**, 7138-7146.
- [6] Atassi, Y. and Tally, M. (2017) Low Sintering Temperature of Mg-Cu-Zn Ferrites Prepared by the Citrate Precursor Method. *Journal of the Iranian Chemical Society*, **3**, 242-246.
- [7] Hakim, M.A., Akhter, S., Paul, D.P. and Hoque, S.M. (2015) Effect of Mg Substituted on Physical and Magnetic Properties of Cu-Mg Ferrites. *Applied Research Journal*, **1**, 91-96.
- [8] Satheeskumar, S., Jeevanantham, V. and Tamilselvi, D. (2018) Effect of Cu-Doping on the Structural and Optical Properties of ZnO Nanocrystallites Prepared by Chemical Precipitation Method. *Journal of Ovonic Research*, **14**, 9-15.
- [9] Zaki, H.M., AL-Henit, S.I., Ahmad, U., AL-Marzouki, F., Abdel-Daiem, A., Elmosalami, T.A., Dawoud, H.A., AL-Hazmi, F.S. and Ata-Aillah, S.S. (2013) Magnesium-Zinc Ferrite Nanoparticles: Effect of Copper Doping on the Structural, Electrical, and Magnetic Properties. *Journal of Nanoscience and Nanotechnology*, **13**, 4056-4065. <https://doi.org/10.1166/jnn.2013.7434>
- [10] Ahamad, H.S., Kakde, A., Meshram, N.S., Rewatkar, K.G. and Dhable, S.J. (2016) Synthesis and Characterization of Nanostructure Copper Ferrites by Microwave Assisted Sol-Gel Auto-Combustion Method. *International Journal of Luminescence and Applications*, **6**, 135-138.
- [11] Thorat, L.M., Patil, J.Y., Nadargi, D.Y., Ghodake, U.R., Kambale, R.C. and Suryavanshi, S.S. (2018) Co^{2+} Substituted Mg-Cu-Zn Ferrite: Evaluation of Structural, Magnetic, and Electromagnetic Properties. *Journal of Advanced Ceramics*, **7**, 207-217. <https://doi.org/10.1007/s40145-018-0272-6>
- [12] Gharibshahian, M., Nourbakhah, M. and Mirzaee, O. (2018) Evaluation of the Superparamagnetic and Biological Properties of Microwave Assisted Synthesized Zn-Cd Doped CoFe_2O_4 Nanoparticles via Pecking Sol-Gel Method. *Journal of Sol-Gel Science and Technology*, **85**, 684-692. <https://doi.org/10.1007/s10971-017-4570-1>
- [13] Ali, B.M., Siddig, M.A., Alsabah, Y.A., Elbadawi, A.A. and Ahmed, A.I. (2018) Effect of Cu^{2+} Doping on Structural and Optical Properties of Synthetic $\text{Zn}_{0.5}\text{Cu}_x\text{Mg}_{0.5-x}\text{Fe}_2\text{O}_4$ ($x= 0.0, 0.1, 0.2, 0.3, 0.4$) Nano-Ferrites. *Advances in Nanoparticles*, **7**, 1-10. <https://doi.org/10.4236/anp.2018.71001>
- [14] Alsabah, Y.A., AlSalhi, M.S., Elbadawi, A.A. and Mustafa, E.M. (2017) Influence of Zn^{2+} and Ni^{2+} Cations on the Structural and Optical Properties of $\text{Ba}_2\text{Zn}_{1-x}\text{Ni}_x\text{WO}_6$ ($0 \leq x \leq 1$) Tungsten Double Perovskites. *Journal of Alloys and Compounds*, **701**, 797-805. <https://doi.org/10.1016/j.jallcom.2017.01.203>
- [15] Alsabah, Y.A., Elbadawi, A.A., Mustafa, E.M. and Siddig, M.A. (2016) The Effect of

- Replacement of Zn^{2+} Cation with Ni^{2+} Cation on the Structural Properties of $Ba_2Zn_{1-x}Ni_xWO_6$ Double Perovskite Oxides ($X = 0, 0.25, 0.50, 0.75, 1$). *Journal of Materials Science and Chemical Engineering*, **4**, 61-70.
<https://doi.org/10.4236/msce.2016.42007>
- [16] Alsabah, Y., Al Salhi, M., Elbadawi, A. and Mustafa, E. (2017) Synthesis and Study of the Effect of Ba^{2+} Cations Substitution with Sr^{2+} Cations on Structural and Optical Properties of $Ba_{2-x}Sr_xZnWO_6$ Double + Perovskite Oxides ($x = 0.00, 0.25, 0.50, 0.7, 1.0$). *Materials*, **10**, 469. <https://doi.org/10.3390/ma10050469>
- [17] Alsabah, Y., Elbadawi, A., Siddig, M.A. and Mohamed, I.M. (2015) Synthesis and Physical Properties of the New Double Perovskite X_2AlVO_6 ($X = Ca, Sr$ and Ba). *International Journal of Science and Nature*, **6**, 56-62.
- [18] Manikandan, A., Judith Vijaya, J., Sundararajan, M., Meganathan, C., John Kennedy, L. and Bououdina, M. (2013) Optical and Magnetic Properties of Mg-Doped $ZnFe_2O_4$ Nanoparticles Prepared by Rapid Microwave Combustion Method. *Super lattice and Microstructures*, **64**, 118-131.
<https://doi.org/10.1016/j.spmi.2013.09.021>
- [19] Rosnan, R.M., Othaman, Z., Hussin, R., Ali, A.A., Samavati, A., Dabagh, S. and Zare, S. (2016) Effects of Mg Substitution on the Structural and Magnetic Properties of $Co_{0.5}Ni_{0.5-x}Mg_xFe_2O_4$ Nanoparticle Ferrites. *Chinese Physics B*, **25**, Article ID: 047501. <https://doi.org/10.1088/1674-1056/25/4/047501>
- [20] Ebraheem, S. and El-Saied, A. (2013) Band Gap Determination from Diffuse Reflectance Measurements of Irradiated Lead Barate Glass System Doped with TiO_2 by Using Diffuse Reflectance Technique. *Materials Sciences and Applications*, **4**, 324-329. <https://doi.org/10.4236/msa.2013.45042>
- [21] Baydogan, N., Ozdurmusoglu, A.T., Cimenoglu, H. and Tugru, C.A.B. (2013) Refractive Index and Extinction Coefficient of $ZnO:Al$ Thin Films Derived by Sol-Gel Dip Coating Technique. *Defect and Diffusion Forum*, **334-335**, 290-293.
<https://doi.org/10.4028/www.scientific.net/DDF.334-335.290>